JACS
JOURNAL OF THE AMERICAN CHEMICAL SOCIETY
Communication
pubs.acs.org/JACS

Control over Hierarchy Levels in the Self-Assembly of Stackable Nanotoroids

Shiki Yagai,*[,†] Mitsuaki Yamauchi,[†] Ai Kobayashi,[†] Takashi Karatsu,[†] Akihide Kitamura,[†] Tomonori Ohba,[‡] and Yoshihiro Kikkawa[§]

[†]Graduate School of Engineering and [‡]Graduate School of Science, Chiba University, 1-33 Yayoi-cho, Inage-ku, Chiba 263-8522, Japan

[§]National Institute of Advanced Industrial Science and Technology (AIST), 1-1-1 Higashi, Tsukuba, Ibaraki 305-8562, Japan

Supporting Information

ABSTRACT: We report a precise control over the hierarchy levels in the outstanding self-organization process shown by chiral azobenzene dimer **1**. This compound forms uniform toroidal nanostructures that can hierarchically organize into chiral nanotubes under the control by temperature, concentration, or light. The nanotubes further organized into supercoiled fibrils, which finally intertwined to form double helices with one-handed helical sense.

Realization of complex self-assembly processes, as those woven by naturally occurring proteins with simply designed artificial molecules, is an important research topic for the development of nanotechnologies based on molecular self-assembly.[1] Not only morphological control of final self-assembled products but also dynamic control of hierarchy levels in the self-assembly by external stimuli might be a challenging issue in this research field.[2] Helical architectures are among the most exciting class of self-assembled morphologies because of their functional and topological uniqueness.[3] However, the elucidation and the dynamic control of hierarchy levels embedded in helical nanoarchitectures remain challenging.[4] Here we report on a hierarchical self-assembly of specifically designed azobenzene dimers into toroidal, tubular, and super-helical nanostructures and on the control of these hierarchy levels by temperature, concentration, and light.

Scheme 1 summarizes the hierarchical self-assembly shown by azobenzene dimer **1**. Two alkoxyazobenzenes functionalized with amide group are dimerized through 3,4,5-(tridodecyloxy)-xylylene linker[5] to afford an asymmetric, cone-shaped molecular structure by folding through $\pi-\pi$ stacking interaction. The presence of amide hydrogen-bonding sites in one-side of the folded molecules prevents antiparallel stacking favored by asymmetric structures, facilitating the formation of toroidal aggregates. The resulting toroidal structures have large π-surfaces on their top and bottom and can hierarchically organize into tubular nanostructures. Chiral substituents were introduced into the amide groups to give chiral assemblies that can be studied by CD spectroscopy.[6]

Compound **1** with *trans* configuration at azobenzene moieties was synthesized according to Scheme S1 and characterized by ^{1}H and ^{13}C NMR spectroscopies and ESI mass spectrometry. Self-aggregates of **1** were prepared in MCH by cooling a hot monomeric solution (90°C, c = 3.0×10^{-4} M) to 20°C. Temperature-dependent UV/vis spectra showed the decrease of the $\pi-\pi^*$ transition of the *trans*-azobenzene moieties at λ_{max} = 356 nm upon cooling below 44°C, which was compensated by a new blue-shifted band at 338 nm. This finding suggests the H-type stacking of the chromophores (Figure 1a). Under room light, *trans*:*cis* ratio of the azobenzene moieties was estimated to be 92:8.[7] CD spectra showed the growth of a positive bisignate Cotton effect with the zero-crossing point at 336 nm (Figure 1d), indicating the chiral exciton coupling of azobenzene chromophores by formation of aggregates denoted as **Agg$_{I}$**.

Upon further cooling the solution below 20°C, the CD intensity further increased, and the spectrum recorded at 0°C featured a negative Cotton effect at 312 nm, a much larger positive one at 337 nm, and a new broad negative one centered at 407 nm (Figure 1c). This result indicates the formation of higher order aggregates denoted as **Agg$_{II}$**. Any substantial contribution of LD to the observed CD signals, from large fibrous assemblies,[8] was clearly excluded by LD measurements as well as the fact that compound **2** displayed totally mirror-image CD signals (Figure

Scheme 1. Schematic Representation of the Hierarchical Self-Assembly of 1

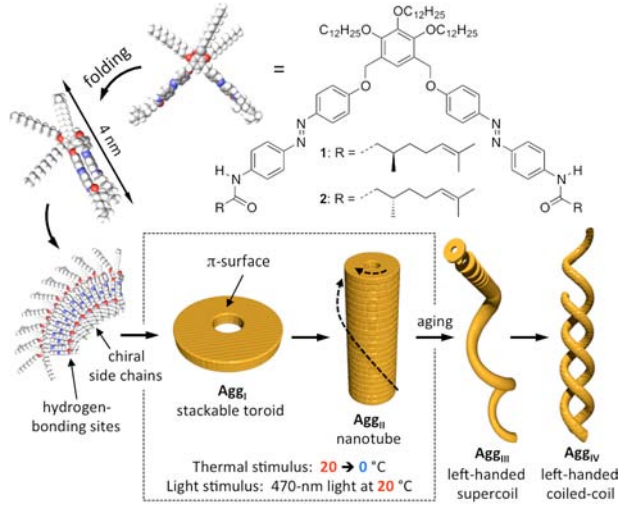

Received: August 28, 2012
Published: October 19, 2012

   dx.doi.org/10.1021/ja308519b | J. Am. Chem. Soc. 2012, 134, 18205−18208

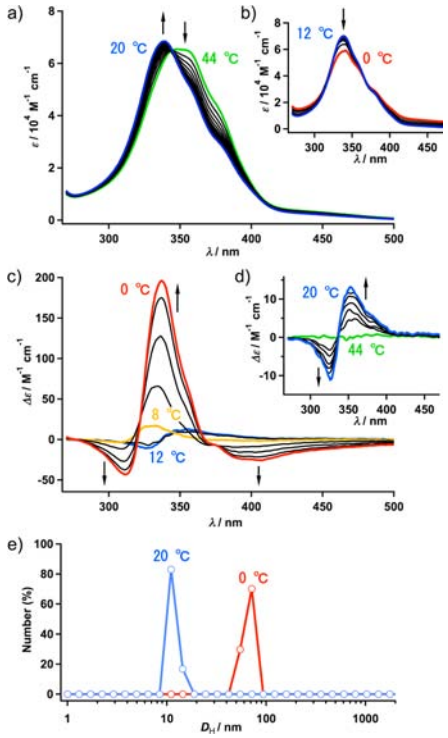

Figure 1. (a,b) UV/vis and (c,d) CD spectra of **1** ($c = 3.0\times10^{-4}$ M) in MCH upon cooling from 90 to 0°C. Arrows indicate changes upon decreasing temperature. (e) DLS of the same solution at 20 (blue) and 0°C (red).

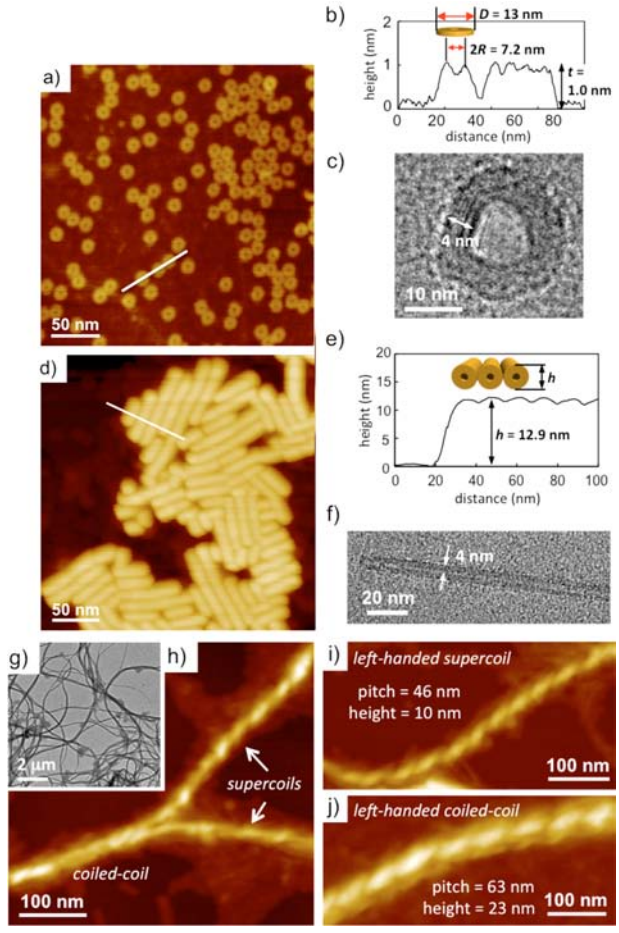

Figure 2. (a,d,h–j) AFM height images, (b,e) AFM cross-sectional analysis along the white lines in (a,d), respectively, and (c,f,g) TEM images of the aggregates of **1** ($c = 3.0\times10^{-4}$ M) formed in MCH at different hierarchy levels. (a–c) Toroidal aggregates $\mathbf{Agg_I}$ formed in MCH at 20°C. (d,e) Tubular aggregates $\mathbf{Agg_{II}}$ formed in MCH at 0°C. Samples were prepared by spin coating the solution. (f) Tubular aggregates $\mathbf{Agg_{II}}$ formed by drop casting $\mathbf{Agg_I}$ solution at 20°C. (g–j) Helical aggregates ($\mathbf{Agg_{III}}$ and $\mathbf{Agg_{IV}}$) precipitated upon aging $\mathbf{Agg_{II}}$ solution for days. Samples were prepared by spin coating the precipitated solution.

S2). Such a CD signal is characteristic of the formation of higher order molecular assemblies involving multiple chiral exciton coupling of the transition-dipole moments.[9] This process was observed as a small decrease of the absorption band by UV/vis spectroscopy. Elevating the solution temperature to 20°C recovered the bisignate Cotton effect, indicating full reversibility between $\mathbf{Agg_I}$ and $\mathbf{Agg_{II}}$. These results demonstrate the presence of thermoreversible chiral supramolecular organization involving the formation of H-aggregates.

DLS experiments provided clear indication for aggregate growth upon lowering the temperature (Figure 1e). At 44°C, no detectable particles (hydrodynamic diameter, $D_H > 1$ nm) were observed by DLS, suggesting a molecularly dissolved state. Upon cooling to 20°C, the particles with average D_H of 11 nm were detected, which upon lowering temperature to 0°C grew up to the aggregates with average D_H of 72 nm. These results support the MCH solution of **1** contains well-defined nanoaggregates, which are visualized by AFM and TEM.

AFM was used to visualize the aggregate nanostructures. To suppress the morphological change induced by evaporation of solvent, the solution of **1** kept at 20°C ($\mathbf{Agg_I}$) was spin coated onto highly oriented pyrolytic graphite (HOPG). Remarkably, uniform toroidal nanostructures were visualized in a wide range of the specimen (Figures 2a and S3). The average top-to-top diameter ($2R$) and thickness (t) of the toroids estimated by cross-sectional analysis are 7.2 ± 0.4 and 1.0 ± 0.1 nm, respectively (Figure 2b), indicating a flat, disk-shaped morphology. By taking tip-broadening effects into account, the average toroid D was estimated as 13 ± 1 nm.[10] TEM of the same sample spin coated onto a carbon-coated copper grid enabled the visualization of an isolated toroid (Figure 2c). The section-width of the toroid was found to be ca. 4 nm, consistent with the folded molecular length of **1** (Scheme 1).

Totally different nanostructures were observed by AFM when the solution of **1** cooled at 0°C ($\mathbf{Agg_{II}}$) was spin coated onto HOPG. As seen in Figures 2d and S4, nanostructures are rod-shaped and polydispersed in the length between 10 and 200 nm. The rods average height (h) is 12.9 ± 0.6 nm (Figure 2e), consistent with the toroid D. Interestingly, the same rod-shaped nanostructures were found when the solution of $\mathbf{Agg_I}$ was drop cast onto HOPG (Figure S5). These results indicate that the toroidal $\mathbf{Agg_I}$ stacks to form rod-shaped $\mathbf{Agg_{II}}$ under more favorable aggregation conditions (lower temperature or higher concentration). TEM observation of the nanorods displayed a bright line running parallel to the long axis (Figure 2f), which is indicative of the formation of a hollow tubular structure (nanotube).[11] Nanotube wall thicknesses are ~4 nm, consistent with the section-width of the toroids.

Tubular nanostructures ($\mathbf{Agg_{II}}$) of **1** could be elongated by aging the solution at 0°C for days, affording insoluble precipitates in the bottom of cuvettes. TEM images of the precipitates

dx.doi.org/10.1021/ja308519b | J. Am. Chem. Soc. 2012, 134, 18205–18208

displayed micrometer-scale fibrous aggregates (Figure 2g). AFM analysis of the smallest-resolved fibers revealed that elongated nanotubes are twisted into left-handed supercoils with helical pitches of ~46 nm and maximum height of 10.3 nm ($\mathbf{Agg}_{III}$, Figure 2i). Furthermore, these fibers are intertwined (Figure 2h) to form left-handed coiled coil structures with helical pitches of ~63 nm and maximum height of 23.1 nm ($\mathbf{Agg}_{IV}$, Figure 2j). No right-handed superhelical structures were found by repeated AFM measurements, indicating molecular chirality is transcribed to nanoscopic chirality even though no chiral morphology is found for intermediate nanostructures.

The results demonstrate that **1** undergoes a remarkable hierarchical self-assembly process (Scheme 1) with unique transcription of molecular to supramolecular chirality. The bisignate CD signal displayed by $\mathbf{Agg}_{I}$ indicates that **1** takes a folded conformation via intramolecular H-type stacking of azobenzene chromophores. This is in sharp contrast to the self-assembly of Würthner's merocyanine dimers where strong dipolar repulsion prevents their folding, leading to extended supramolecular polymerization.[5,9c] In the present system such folded molecules are considered to further aggregate mainly by H-bonding interactions and may not be reflected in UV/vis and CD properties. The presence of amide functionality on one side of the folded molecules, plus their asymmetric structure, could induce a curvature in the aggregates, leading to formation of toroidal nanostructures ($\mathbf{Agg}_{I}$). Involvement of H-bonding interactions was confirmed by IR measurements (Figure S6).[12] Toroidal nanostructures formed by this mechanism should have large π-surfaces, which is in sharp contrast to previously reported discrete nanorings fully surrounded by aliphatic chains.[13] Thus, toroids can further stack to form nanotubes ($\mathbf{Agg}_{II}$) under appropriate conditions.[14] Induction of strong CD signals is rationalized by the presence of a large amount of chiral side chains directed toward the center of the toroids, inducing strong helical bias in the rotational displacement upon stacking. The resulting tubular structure with one-handed helical chirality would gain in strain energy upon elongation, which is canceled by formation of supercoiled structures ($\mathbf{Agg}_{II}\rightarrow\mathbf{Agg}_{III}$, Scheme 1). Left-handed supercoils further merge to form left-handed coiled coil structures ($\mathbf{Agg}_{IV}$).[15]

Irradiation of the MCH solution of $\mathbf{Agg}_{I}$ formed at 20°C with 365 nm UV light (38 mW/cm^2 LED lamp) caused a smooth decrease of the absorption band at 338 nm and an increase of a new band at ~450 nm, indicating *trans*-to-*cis* isomerization of the azobenzene chromophores (Figure 3a). In Figure 3e, the *cis*:*trans* ratio (left axis) and the CD activity (right axis) are plotted versus UV and visible light irradiation time with the photoresponsive self-assembly of **1**. The *cis*:*trans* ratio at the photostationary state (PSS) was roughly estimated to be 15:85, indicating that most of **1** possess two or one nonaggregative *cis*-azobenzene moieties.[16,17] The CD spectrum recorded at the PSS displayed no Cotton effect (Figure 3c). DLS measurements did not show the presence of any substantial particles, indicating $\mathbf{Agg}_{I}$ photodisruption to the monomeric level by the transformation of molecular shapes. This was further confirmed by AFM study showing the disappearance of toroidal nanostructures for spin-coated samples.

Irradiation of the *cis*-rich solution with 470 nm visible light (18 mW/cm^2 LED lamp) induced a smooth *cis*-to-*trans* isomerization, and the 40 s irradiation resulted in the *trans*:*cis* ratio of 77:23 (Figure 3b,e). CD spectrum showed the recovery of the bisignate Cotton effect characteristic of $\mathbf{Agg}_{I}$ (Figure 3d). Surprisingly, further irradiation with 470 nm light for 80 s (total

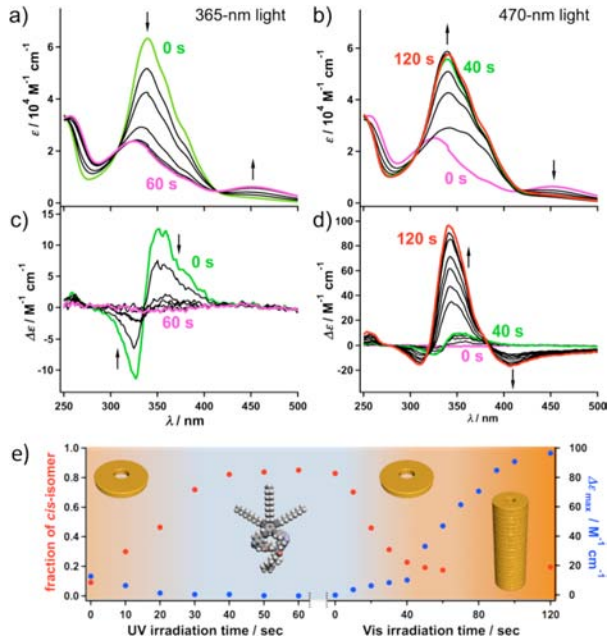

Figure 3. Photoinduced (a,b) UV/vis and (c,d) CD spectral change of **1** ($c = 3.0\times10^{-4}$ M) in MCH at 20°C. (a,c) Changes upon irradiation of a *trans*-rich solution with 365 nm UV light. (b,d) Changes upon irradiation of the *cis*-rich solution with 470 nm visible light. (e) Plots of the fraction of *cis*-azobenzene moieties (red marks, left axis) and maximum $\Delta\varepsilon$ values (blue marks, right axis) versus irradiation time of the UV (left side) and visible (right side) lights. Aggregation states are shown with gradated background colors representing monomeric (water blue) and aggregated (orange) states.

120 s) induced strong CD signals characteristic of the formation of $\mathbf{Agg}_{II}$ even at 20°C (red curve, Figure 3d), while UV/vis spectra showed a marginal increase of the absorption band of the *trans*-azobenzene moiety (red curve, Figure 3b). This situation is totally different from the system under room light, where the hierarchical growth of $\mathbf{Agg}_{I}\rightarrow\mathbf{Agg}_{II}$ starts below 8°C (Figure 1b). Removal of the 470 nm visible light resulted in a smooth decrease of the strong CD band within 5 min to recover the bisignate Cotton effect. As a control experiment, we irradiated $\mathbf{Agg}_{I}$ prepared by cooling procedure with the same light source. Also in this case, the transition to $\mathbf{Agg}_{II}$ was confirmed by the growth of the strong CD signals even at 20°C. These observations clearly demonstrate that toroidal aggregates $\mathbf{Agg}_{I}$, whether formed by temperature or light, are stimulated to stack into tubular aggregates $\mathbf{Agg}_{II}$ upon 470 nm light exposure.

At the moment we cannot propose a rational mechanism for the above photoinduced $\mathbf{Agg}_{I}\rightarrow\mathbf{Agg}_{II}$ transition; such a transition could be caused by a slight decrease of nonaggregative *cis*-azobenzene moieties in an already *trans*-rich solution upon exposure to the strong visible light >40 s (Figure 3e). However, the content of *cis*-azobenzene moieties did not go below 17% by prolonged irradiation, which is greater than that of the initial $\mathbf{Agg}_{I}$ solution under room light (8%). CD spectroscopy also confirmed that almost complete thermal elimination of the *cis*-azobenzene moieties in darkness for 24 h does not induce $\mathbf{Agg}_{I}\rightarrow\mathbf{Agg}_{II}$ transition at 20°C.

Recently, Ajayaghosh et al. reported that UV light irradiation of a π-extended azobenzene compound results in the growth of aggregates from nanodots to nanorods due to the dipole-assisted particle growth induced by polar *cis*-azobenzene moieties generated to a small extent on the aggregate surface.[2c] In our

dx.doi.org/10.1021/ja308519b | J. Am. Chem. Soc. 2012, 134, 18205−18208

system, irradiation of **1** with UV light quantitatively converted aggregative *trans*-azobenzene moieties to nonaggregative *cis*-isomers (Figure 3a), collapsing almost all aggregates to monomers (DLS study). However, the different situation may be achieved when **1** is irradiated with visible light at 470 nm: the reversible *trans-cis* isomerization of the azobenzene moieties can be promoted because both isomers have absorption at 470 nm, while the fraction of aggregative *trans*-isomer is kept in large excess because the *cis*-isomer has a greater molar extinction coefficient at this wavelength (Figure 3b). In this situation, a rapid generation and evanescence of polar *cis*-azobenzene moieties could occur within the toroidal aggregates. This is capable of promoting hierarchical growth of the aggregates by increasing nanostructure surface polarity in nonpolar environments; verification is ongoing.

In summary, azobenzene dimer **1** showed a remarkably defined hierarchical self-assembly process that enables us to acquire the snapshots of nanoscale morphologies generated in each hierarchy level by modulating external environments, such as temperature, concentration, and light. Our study illustrated that even in nonaqueous media, rather simple artificial small molecular building blocks could achieve complex hierarchical organization processes, as those shown by biological systems, such as tobacco mosaic virus proteins. It was also implied that various helical assemblies reported so far might be constructed along with more complicated self-organization schemes than expected. Regarding the present system, elucidation of the mechanism of hierarchical transfer of the molecular chirality to the supramolecular chirality and phototriggered stacking of toroidal aggregates remain formidable challenges.

■ ASSOCIATED CONTENT

Ⓢ Supporting Information

Experimental details and characterization data. This material is available free of charge via the Internet at http://pubs.acs.org.

■ AUTHOR INFORMATION

Corresponding Author

yagai@faculty.chiba-u.jp

Notes

The authors declare no competing financial interest.

■ ACKNOWLEDGMENTS

Work was partially supported by Core Research for Evolutional Science and Technology, JST. TEM was conducted at Chiba University.

■ REFERENCES

(1) (a) Whitesides, G. M.; Grzybowski, B. *Science* **2002**, *295*, 2418. (b) Rosen, B. M.; Wilson, C. J.; Wilson, D. A.; Peterca, M.; Imam, M. R.; Percec, V. *Chem. Rev.* **2009**, *109*, 6275. (c) Hoeben, F. J. M.; Jonkheijm, P.; Meijer, E. W.; Schenning, A. P. H. J. *Chem. Rev.* **2005**, *105*, 1491.

(2) (a) Coleman, A. C.; Beierle, J. M.; Stuart, M. C. A.; Macia, B.; Caroli, G.; Mika, J. T.; van Dijken, D. J.; Chen, J.; Browne, W. R.; Feringa, B. L. *Nat. Nanotechnol.* **2011**, *6*, 547. (b) Muraoka, T.; Cui, H.; Stupp, S. I. *J. Am. Chem. Soc.* **2008**, *130*, 2946. (c) Mahesh, S.; Gopal, A.; Thirumalai, R.; Ajayaghosh, A. *J. Am. Chem. Soc.* **2012**, *134*, 7227. (d) Yagai, S.; Ohta, K.; Gushiken, M.; Iwai, K.; Asano, A.; Seki, S.; Kikkawa, Y.; Morimoto, M.; Kitamura, A.; Karatsu, T. *Chem.—Eur. J.* **2012**, *18*, 2244.

(3) (a) Rowan, A. E.; Nolte, R. J. M. *Angew. Chem., Int. Ed.* **1998**, *37*, 63. (b) Brizard, A.; Oda, R.; Huc, I. *Top. Curr. Chem.* **2005**, *256*, 167. (c) Amabilino, D. B. *Chirality at the Nanoscale*; Wiley-VCH: Weinheim, 2009. (d) *Supramolecular Chirality*; Crego-Calama, M.; Reinhoudt, D. N., Ed.; Topics in Current Chemistry 265, Springer, Berlin, 2006. (e) Palmans, A. R. A.; Meijer, E. W. *Angew. Chem., Int. Ed.* **2007**, *46*, 8948. (f) Praveen, V. K.; Babu, S. S.; Vijayakumar, C.; Varghese, R.; Ajayaghosh, A. *Bull. Chem. Soc. Jpn.* **2008**, *81*, 1196.

(4) For examples: (a) Engelkamp, H.; Middelbeek, S.; Nolte, R. J. M. *Science* **1999**, *284*, 785. (b) Li, L.-s.; Jiang, H.; Messmore, B. W.; Bull, S. R.; Stupp, S. I. *Angew. Chem., Int. Ed.* **2007**, *46*, 5873. (c) Iwaura, R.; Shimizu, T. *Angew. Chem., Int. Ed.* **2006**, *45*, 4601.

(5) (a) Würthner, F.; Yao, S.; Beginn, U. *Angew. Chem., Int. Ed.* **2003**, *42*, 3247. (b) Yao, S.; Beginn, U.; Gress, T.; Lysetska, M.; Würthner, F. *J. Am. Chem. Soc.* **2004**, *126*, 8336.

(6) (a) Berova, N.; Nakanishi, K. *In Circular DichroismsPrinciples and Application*, 2nd ed.; Berova, N., Nakanishi, K., Woody, R. W., Eds; Wiley-VCH: New York, 2000; Chpt 12. (b) Gottarelli, G.; Lena, S.; Masiero, S.; Pieraccini, S.; Spada, G. P. *Chirality* **2008**, *20*, 471.

(7) For details see SI.

(8) (a) Wolffs, M.; George, S. J.; Tomovic, Z.; Meskers, S. C. J.; Schenning, A. P. H. J.; Meijer, E. W. *Angew. Chem., Int. Ed.* **2007**, *46*, 8203. (b) Tsuda, A.; Alam, M. A.; Harada, T.; Yamaguchi, T.; Ishii, N.; Aida, T. *Angew. Chem., Int. Ed.* **2007**, *46*, 8198.

(9) (a) Pawlik, A.; Kirstein, S.; De Rossi, U.; Daehne, S. *J. Phys. Chem. B* **1997**, *101*, 5646. (b) Didraga, C.; Klugkist, J. A.; Knoester, J. *J. Phys. Chem. B* **2002**, *106*, 11474. (c) Lohr, A.; Lysetska, M.; Würthner, F. *Angew. Chem., Int. Ed.* **2005**, *44*, 5071.

(10) Samori, P.; Francke, V.; Mangel, T.; Müllen, K.; Rabe, J. P. *Opt. Mater.* **1998**, *9*, 390.

(11) (a) Shimizu, T.; Masuda, M.; Minamikawa, H. *Chem. Rev.* **2005**, *105*, 1401. (b) Hill, J. P.; Jin, W.; Kosaka, A.; Fukushima, T.; Ichihara, H.; Shimomura, T.; Ito, K.; Hashizume, T.; Ishii, N.; Aida, T. *Science* **2004**, *304*, 1481. (c) von Berlepsch, H.; Kirstein, S.; Böttcher, C. *J. Phys. Chem. B* **2003**, *107*, 9646.

(12) FTIR spectra of a dried film of **1** showed NH stretching band at 3315 cm^{-1}, suggesting amides are involved in H-bonding.

(13) (a) Yagai, S.; Mahesh, S.; Kikkawa, Y.; Unoike, K.; Karatsu, T.; Kitamura, A.; Ajayaghosh, A. *Angew. Chem., Int. Ed.* **2008**, *47*, 4691. (b) Yagai, S.; Kubota, S.; Saito, H.; Unoike, K.; Karatsu, T.; Kitamura, A.; Ajayaghosh, A.; Kanesato, M.; Kikkawa, Y. *J. Am. Chem. Soc.* **2009**, *131*, 5408. (c) Yagai, S.; Aonuma, H.; Kikkawa, Y.; Kubota, S.; Karatsu, T.; Kitamura, A.; Mahesh, S.; Ajayaghosh, A. *Chem.—Eur. J.* **2010**, *16*, 8652. (d) Yagai, S.; Goto, Y.; Xu, L.; Karatsu, T.; Kitamura, A.; Kuzuhara, D.; Yamada, H.; Kikkawa, Y.; Saeki, A.; Seki, S. *Angew. Chem., Int. Ed.* **2012**, *51*, 6643.

(14) Most self-assembled nanotubes are formed directly from small molecular building blocks, but several systems revealed the presence of intermediate toroidal nanostructures: (a) Shao, H.; Seifert, J.; Romano, N. C.; Gao, M.; Helmus, J. J.; Jaroniec, C. P.; Modarelli, D. A.; Parquette, J. R. *Angew. Chem., Int. Ed.* **2010**, *49*, 7688. (b) Tu, S.; Kim, S. H.; Joseph, J.; Modarelli, D. A.; Parquette, J. R. *J. Am. Chem. Soc.* **2011**, *133*, 19125. (c) Chandrasekhar, N.; Chandrasekar, R. *Angew. Chem., Int. Ed.* **2012**, *51*, 3556.

(15) (a) Würthner, F.; Chen, Z.; Hoeben, F. J. M.; Osswald, P.; You, C.-C.; Jonkheijm, P.; Herrikhuyzen, J. V.; Schenning, A. P. H. J.; van der Schoot, P. P. A. M.; Meijer, E. W.; Beckers, E. H. A.; Meskers, S. C. J.; Janssen, R. A. J. *J. Am. Chem. Soc.* **2004**, *126*, 10611. (b) Danila, I.; Riobé, F. o.; Piron, F.; Puigmartí-Luis, J.; Wallis, J. D.; Linares, M.; Ågren, H.; Beljonne, D.; Amabilino, D. B.; Avarvari, N. *J. Am. Chem. Soc.* **2011**, *133*, 8344.

(16) (a) Murata, K.; Aoki, M.; Suzuki, T.; Harada, T.; Kawabata, H.; Komori, T.; Ohseto, F.; Ueda, K.; Shinkai, S. *J. Am. Chem. Soc.* **1994**, *116*, 6664. (b) Kawasaki, T.; Tokuhiro, M.; Kimizuka, N.; Kunitake, T. *J. Am. Chem. Soc.* **2001**, *123*, 6792. (c) Yagai, S.; Nakajima, T.; Karatsu, T.; Saitow, K.; Kitamura, A. *J. Am. Chem. Soc.* **2004**, *126*, 11500. (d) Yagai, S.; Nakajima, T.; Kishikawa, K.; Kohmoto, S.; Karatsu, T.; Kitamura, A. *J. Am. Chem. Soc.* **2005**, *127*, 11134.

(17) Reviews: (a) Yagai, S.; Kitamura, A. *Chem. Soc. Rev.* **2008**, *37*, 1520. (b) Yagai, S.; Karatsu, T.; Kitamura, A. *Chem.—Eur. J.* **2005**, *11*, 4054.